

## Noninteracting-spin band model for dielectric screening and local field corrections in ferromagnetic nickel

Natthi Singh, Joginder Singh, and Satya Prakash

Physics Department, Panjab University, Chandigarh-160014, India

(Received 25 July 1974)

The diagonal and the nondiagonal parts of the dielectric matrix are evaluated for ferromagnetic nickel using a noninteracting-spin band model which is constructed with the help of the detailed band-structure calculations of Callaway and Wang. The free-electron approximation is used for the electrons in the  $s$  band, while the simple tight-binding wave function is used for electrons in the  $d$  subbands. The calculations for the diagonal part are performed for the field vector  $\vec{q}$  along the three principal symmetry directions [100], [110], and [111] and the anisotropy is found to be quite small. Outside the first Brillouin zone, the calculations are performed only along the [001] direction for both diagonal and nondiagonal parts. The contribution of minority-spin ( $\downarrow$ ) bands is found to be much larger as compared to the contribution of majority-spin ( $\uparrow$ ) bands. Away from the vicinity of  $\vec{q} = 0$  the contribution due to interband transitions is found to be much smaller as compared to the contribution due to intraband transitions. The nondiagonal part, i.e., the local-field corrections for interband and intraband transitions are found to be 50% of the diagonal parts for the intermediate values of  $|\vec{q} + \vec{G}|$ , where  $\vec{G}$  is a reciprocal-lattice vector. The total diagonal part of the dielectric function is also compared with the results for the paramagnetic phase and it is found that the dielectric function is slightly larger for the paramagnetic phase.

### I. INTRODUCTION

The formal microscopic theory of dielectric screening in solids has been discussed by Adler,<sup>1</sup> Wiser,<sup>2</sup> and Ehrenreich and Cohen.<sup>3</sup> Sinha *et al.*<sup>4,5</sup> proposed a factorization *Ansatz* for the dielectric matrix which allows one to invert it exactly and to take into account the effect of the local-field correction, which is a manifestation of the off-diagonal part of the dielectric matrix. These authors made an extensive analysis of the dielectric matrix for insulators and found that it leads to correct analytic behavior as the field wave vector  $\vec{q} \rightarrow 0$ . In simple metals the free-electron approximation is fairly valid, and therefore the dielectric matrix becomes diagonal. In transition metals the conduction electrons are neither totally free nor completely bound. An appropriate wave function for conduction electrons in these metals should include both the plane-wave and the tight-binding parts. Therefore a self-consistent treatment of the electron density response function will include both the diagonal and the nondiagonal parts of the dielectric matrix. Hayashi and Shimizu<sup>6</sup> derived a generalized dielectric function for a single-band model of  $d$  electrons and for a two-band model of  $d$  and  $s$  electrons and applied it to calculating the impurity screening and the induced spin density of ferromagnetic nickel by using the effective-mass approximation for the energy bands.

Earlier, Prakash and Joshi<sup>7</sup> (PJ) proposed a

noninteracting band model for  $s$  and  $d$  conduction electrons in transition metals and applied it to calculating the diagonal part of the dielectric matrix for paramagnetic nickel<sup>7</sup> for the configuration  $(3d)^9(4s)^1$  and  $(3d)^9(4s)^0$ .<sup>6</sup> The model was applied to calculating the phonon frequencies of paramagnetic nickel<sup>8</sup> for both configurations. Hanke and Bilz<sup>9</sup> and Hanke<sup>10</sup> justified the above model in the Wannier representation neglecting the  $s$ - $d$  hybridization which happens only in a small region of momentum space and much below the Fermi energy. Hanke<sup>11</sup> extended the calculations for phonon frequencies of paramagnetic nickel and palladium using the intraband part of the dielectric function. The interband part of the dielectric function has been neglected in the above calculations because of its smallness, but this may not be true in general for other transition metals such as chromium.<sup>12</sup>

In this paper the noninteracting band model is extended for ferromagnetic nickel. The calculations for the diagonal and nondiagonal parts of the dielectric matrix, which include both intraband and interband transitions, are carried out. A complete inversion of the dielectric matrix and the calculations of phonon frequencies for ferromagnetic nickel for which experimental data are available<sup>13</sup> will be reported in a subsequent paper. The plan of this paper is as follows: The noninteracting-spin band model is discussed in Sec. II; the formalism is given in Sec. III; the results are presented in Sec. IV and discussed in Sec. V.

## II. NONINTERACTING-SPIN BAND MODEL

Energy-band calculations for ferromagnetic nickel have been done by several authors.<sup>14</sup> We use the recent calculations of Callaway and Wang to construct the noninteracting-spin band model as discussed by PJ. Calculations for isotropic energy bands are carried out separately for majority and minority spins and these energy bands are shown in Fig. 1. The Fermi momentum and the average effective masses are tabulated in Tables I and II, and the other parameters are the same as in PJ. The energies are measured in rydbergs and the distances are measured in bohr units. The Brillouin zone is replaced by an equivalent sphere. All the majority-spin  $d$  sub-bands are completely filled, but the  $s$  band is partially filled, while the minority-spin two  $d$  sub-bands and  $s$  band are partially filled. The partially filled  $d$  sub-bands are assigned the magnetic quantum numbers  $m=1$  and  $2$ , as discussed in PJ. The filled minority-spin  $d$  sub-bands are shifted upwards with respect to the majority-spin  $d$  sub-bands by about 0.05 Ryd at the center of the zone and at the zone boundary. This is in agreement with the detailed calcu-

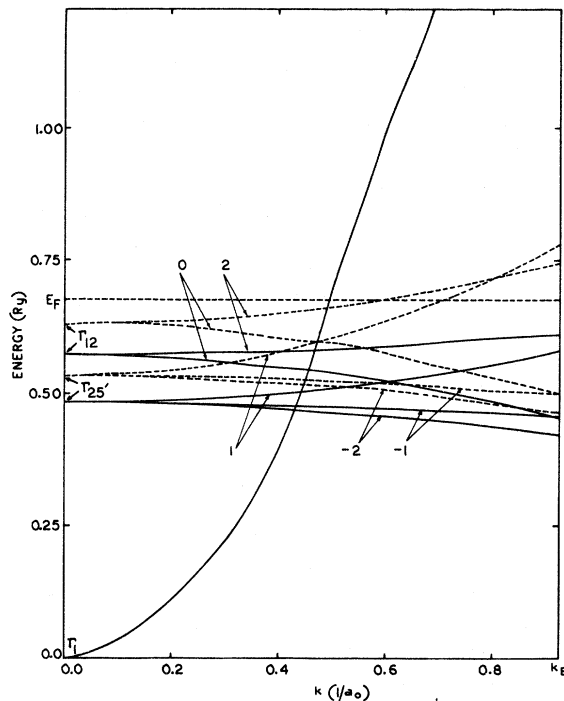


FIG. 1. Isotropic energy-band structure for ferromagnetic nickel. The solid lines represent the band structure for the majority spins while the dashed lines represent the band structure for minority spins. The numbers written therein denote the magnetic quantum number  $m$  assigned to them.  $k_B$  is Brillouin-sphere radius.

TABLE I. Fermi momentum and effective masses for partially filled  $s$  and  $d$  sub-bands. Here  $a_0$  is the Bohr radius.

Fermi momentum for $s$ bands (in units of $1/a_0$ )	$k_{FS\uparrow}$	0.6221
	$k_{FS\downarrow}$	0.6221
Effective masses for $s$ bands (in a.u.)	$m_{s\uparrow}$	0.5733
	$m_{s\downarrow}$	0.5725
Fermi momentum for partially filled $d$ sub-bands (in units of $1/a_0$ )	$k_{Fd1\downarrow}$	0.8892
	$k_{Fd2\downarrow}$	0.7489
Effective masses for partially filled $d$ sub-bands (in a.u.)	$m_{d1\downarrow}$	5.5681
	$m_{d2\downarrow}$	11.9330

lations of Callaway and Wang. For the magnetic configuration  $(3d)^{9.4}(4s)^{0.6}$  each  $s$  band is assigned with 0.3 electron per atom and the remaining 1.4 electrons are distributed in  $m=1$  and  $2$  minority-spin  $d$  sub-bands. Let these two  $d$  sub-bands cross the Fermi energy at the distances  $k_1$  and  $k_2$  from the origin, respectively. The volumes occupied by these bands are  $\frac{4}{3}\pi k_1^3$  and  $\frac{4}{3}\pi k_2^3$ . We distribute the 1.4 electrons according to the ratio of volume occupied by these bands and find 0.88 and 0.52 electron per atom in the  $m=1$  and  $2$   $d$  sub-bands, respectively.

In the noninteracting-spin band model the electrons will readjust themselves through the ionic motion which is due to the thermal field by the following transitions: (i) intraband transitions in partially filled majority- and minority-spin  $s$  bands; (ii) interband transitions from filled majority-spin  $d$  sub-bands to the partially filled majority-spin  $s$  band; (iii) intraband transitions in partially filled minority-spin  $d$  sub-bands and interband transitions from partially and completely filled minority-spin  $d$  sub-bands to partially filled minority spin  $s$  and  $d$  sub-bands; (iv) interband transitions from the partially filled minority-spin  $s$  band to partially filled minority-spin  $d$  sub-bands.

## III. THEORY

The generalized spin-dependent dielectric matrix obtained self-consistently<sup>3</sup> in the Hartree approximation is

TABLE II. Average effective masses (in a.u.) for filled  $d$  sub-bands.

$m$	1	2	0	-1	-2
$m_{dm\uparrow}$	9.0164	22.7694	-7.2480	-30.8452	-14.8412
$m_{dm\downarrow}$	...	...	-6.7295	-25.6972	-12.6470

$$\begin{aligned}
& \epsilon(\vec{q} + \vec{G}, \vec{q} + \vec{G}') \\
&= \delta_{G G'} - v(\vec{q} + \vec{G}) \sum_{lm\sigma} \sum_{l'm'\sigma'} \frac{n_{lm\sigma}(\vec{k}) - n_{l'm'\sigma'}(\vec{k}')}{E_{lm\sigma}(\vec{k}) - E_{l'm'\sigma'}(\vec{k}')} \\
&\quad \times \langle \psi_{lm\sigma}(\vec{k}) | e^{-i(\vec{q} + \vec{G}) \cdot \vec{r}} | \psi_{l'm'\sigma'}(\vec{k}') \rangle \\
&\quad \times \langle \psi_{l'm'\sigma'}(\vec{k}') | e^{i(\vec{q} + \vec{G}') \cdot \vec{r}} | \psi_{lm\sigma}(\vec{k}) \rangle. \tag{1}
\end{aligned}$$

Here  $\psi_{lm\sigma}(\vec{k})$  and  $E_{lm\sigma}(\vec{k})$  are the eigenfunction and the eigenvalue for the electron with wave vector  $\vec{k}$ .  $l$ ,  $m$ , and  $\sigma$  are orbital, magnetic, and spin quantum numbers, respectively, and act as the band indices.  $n_{lm\sigma}(\vec{k})$  is the Fermi occupation-probability function, which is unity if the state is occupied, otherwise zero.  $\vec{G}$  and  $\vec{G}'$  are reciprocal-lattice vectors and  $v(\vec{q})$  is the Fourier transform of the electron-electron Coulomb interaction. The electron wave vectors  $\vec{k}$  and  $\vec{k}'$  ( $=\vec{k} + \vec{q}$ ) lie in the first Brillouin zone. Because of the orthogonality of the spin functions, Eq. (1) simplifies as

$$\begin{aligned}
& \epsilon(\vec{q} + \vec{G}, \vec{q} + \vec{G}') \\
&= \delta_{G G'} - v(\vec{q} + \vec{G}) [\chi_{\uparrow\uparrow}^0(\vec{q} + \vec{G}, \vec{q} + \vec{G}') \\
&\quad + \chi_{\downarrow\downarrow}^0(\vec{q} + \vec{G}, \vec{q} + \vec{G}')], \tag{2}
\end{aligned}$$

where

$$\begin{aligned}
\chi_{\alpha\sigma}^0 &= \sum_{lm} \sum_{l'm'} \sum_{kk'} \frac{n_{lm\sigma}(\vec{k}) - n_{l'm'\sigma}(\vec{k}')}{E_{lm\sigma}(\vec{k}) - E_{l'm'\sigma}(\vec{k}')} \\
&\quad \times \langle \psi_{lm\sigma}(\vec{k}) | e^{-i(\vec{q} + \vec{G}) \cdot \vec{r}} | \psi_{l'm'\sigma}(\vec{k}') \rangle \\
&\quad \times \langle \psi_{l'm'\sigma}(\vec{k}') | e^{i(\vec{q} + \vec{G}') \cdot \vec{r}} | \psi_{lm\sigma}(\vec{k}) \rangle. \tag{3}
\end{aligned}$$

$\chi_{\uparrow\uparrow}^0$  and  $\chi_{\downarrow\downarrow}^0$  are the charge susceptibility functions for the up- and down-spin electrons, respectively. Symbolically, in terms of the contributions to the dielectric matrix from various intra- and inter-band transitions, we can write Eq. (1)

$$\begin{aligned}
& \epsilon(\vec{q} + \vec{G}, \vec{q} + \vec{G}') \\
&= \delta_{G G'} - \sum_{\sigma} [\epsilon_{ss}^{\sigma}(\vec{q} + \vec{G}, \vec{q} + \vec{G}') + \epsilon_{dd}^{\sigma}(\vec{q} + \vec{G}, \vec{q} + \vec{G}') \\
&\quad + \epsilon_{ds}^{\sigma}(\vec{q} + \vec{G}, \vec{q} + \vec{G}') + \epsilon_{sd}^{\sigma}(\vec{q} + \vec{G}, \vec{q} + \vec{G}')]. \tag{4}
\end{aligned}$$

Here  $\epsilon_{ss}^{\sigma}$ ,  $\epsilon_{dd}^{\sigma}$ ,  $\epsilon_{ds}^{\sigma}$ , and  $\epsilon_{sd}^{\sigma}$  correspond to  $s$ -band-to- $s$ -band,  $d$ -sub-bands-to- $d$ -sub-bands,  $d$ -sub-bands-to- $s$ -band, and  $s$ -band-to- $d$ -sub-bands transitions, respectively. The expressions for  $\epsilon_{ss}^{\sigma}$ ,  $\epsilon_{dd}^{\sigma}$ ,  $\epsilon_{ds}^{\sigma}$ , and  $\epsilon_{sd}^{\sigma}$  are evaluated similarly as that in PJ. We briefly review the formalism here for the sake of completeness. Using the free-electron approximation for the wave function and the parabolic-band approximation for the energies of the electrons in the  $s$  band, we obtain the well-known expression for  $\epsilon_{ss}^{\sigma}$ :

$$\begin{aligned}
& \epsilon_{ss}^{\sigma}(\vec{q} + \vec{G}) \\
&= -\frac{m_{s\sigma} k_{F s\sigma} e^2}{\pi \hbar^2 |\vec{q} + \vec{G}|^2} \left( 1 + \frac{4k_{F s\sigma}^2 - |\vec{q} + \vec{G}|^2}{4k_{F s\sigma} |\vec{q} + \vec{G}|} \right. \\
&\quad \left. \times \ln \left| \frac{2k_{F s\sigma} + |\vec{q} + \vec{G}|}{2k_{F s\sigma} - |\vec{q} + \vec{G}|} \right| \right). \tag{5}
\end{aligned}$$

Here  $m_{s\sigma}$  and  $k_{F s\sigma}$  are the effective mass and Fermi momentum for the  $s$  electrons in the  $\sigma$  spin band and  $e$  is the electronic charge.  $\epsilon_{ss}^{\sigma}(\vec{q} + \vec{G})$  is diagonal and does not give rise to the local-field corrections.

Using a simple tight-binding wave function and the parabolic-energy-band approximation for electrons in  $d$  sub-bands, the expression for  $\epsilon_{dd}^{\sigma}(\vec{q} + \vec{G}, \vec{q} + \vec{G}')$  simplifies to

$$\begin{aligned}
& \epsilon_{dd}^{\sigma}(\vec{q} + \vec{G}, \vec{q} + \vec{G}') \\
&= 2v(\vec{q} + \vec{G}) \sum_m \sum_{m'} \Delta_{dm, dm'}^{\sigma}(\vec{q} + \vec{G}) \Delta_{dm, dm'}^{*\sigma}(\vec{q} + \vec{G}') \\
&\quad \times \sum_k \frac{n_{dm\sigma}(\vec{k})}{E_{dm\sigma}(\vec{k}) - E_{dm'\sigma}(\vec{k} + \vec{q})}, \tag{6}
\end{aligned}$$

provided overlapping between  $d$ -wave functions on different lattice sites is assumed to be negligible and only the normal-process contribution is retained. Here the matrix elements are

$$\Delta_{dm, dm'}^{\sigma}(\vec{q} + \vec{G}) = \int \phi_{dm\sigma}^*(\vec{r}) e^{-i(\vec{q} + \vec{G}) \cdot \vec{r}} \phi_{dm'\sigma}(\vec{r}) d\vec{r},$$

and  $\phi_{dm\sigma}(\vec{r})$  are the atomic orbitals. Replacing the sum over  $\vec{k}$  by an integration in Eq. (6), we get

$$\begin{aligned}
& \epsilon_{dd}^{\sigma}(\vec{q} + \vec{G}, \vec{q} + \vec{G}') \\
&= -\frac{e^2}{\pi \hbar^2 |\vec{q} + \vec{G}|^2} \sum_m m_{dm\sigma} k_{F dm\sigma} \Delta_{dm, dm}^{\sigma}(\vec{q} + \vec{G}) \\
&\quad \times \Delta_{dm, dm}^{*\sigma}(\vec{q} + \vec{G}') \left( 1 + \frac{4k_{F dm\sigma}^2 - q^2}{4k_{F dm\sigma} q} \ln \left| \frac{2k_{F dm\sigma} + q}{2k_{F dm\sigma} - q} \right| \right) \\
&\quad \text{for } m = m', \tag{7} \\
&= \frac{4e^2}{\pi \hbar^2 |\vec{q} + \vec{G}|^2} \sum_m \sum_{m'} m_{dm'\sigma} \Delta_{dm, dm'}^{\sigma}(\vec{q} + \vec{G}) \\
&\quad \times \Delta_{dm, dm'}^{*\sigma}(\vec{q} + \vec{G}') [I'(q) + I''(q)] \text{ for } m \neq m', \tag{8}
\end{aligned}$$

where  $I'(q)$  and  $I''(q)$  are the same as defined in PJ. The analytical expressions for  $\Delta_{dm, dm'}^{\sigma}(\vec{q} + \vec{G})$  are evaluated as discussed in PJ. Watson's neutral-atom  $3d$  radial wave function is used in the present calculation, and therefore the matrix elements  $\langle \psi_{lm\sigma}(\vec{k}) | e^{i(\vec{q} + \vec{G}) \cdot \vec{r}} | \psi_{l'm'\sigma}(\vec{k} + \vec{q}) \rangle$  become the same for both the up- and down-spin electrons while the energy-dependent part of the dielectric matrix remains spin dependent. Equation (6) consists of both diagonal and nondiagonal parts, with

local-field corrections arising from the latter.

Using free-electron and simple tight-binding wave functions for  $s$  and  $d$  electrons, respectively, and retaining only the normal-process contribution, the expression for  $\epsilon_{ds}^{\sigma}$  becomes

$$\begin{aligned} \epsilon_{ds}^{\sigma}(\vec{q} + \vec{G}, \vec{q} + \vec{G}') &= v(\vec{q} + \vec{G}) \sum_k \sum_m \frac{n_{dm\sigma}(\vec{k}) - n_{s\sigma}(\vec{k} + \vec{q})}{E_{dm\sigma}(\vec{k}) - E_{s\sigma}(\vec{k} + \vec{q})} \\ &\times \frac{1}{\Omega_0} \int \phi_{dm\sigma}^*(\vec{r}) e^{i(\vec{k} - \vec{G}) \cdot \vec{r}} d\vec{r} \\ &\times \int \phi_{dm\sigma}(\vec{r}) e^{-i(\vec{k} - \vec{G}') \cdot \vec{r}} d\vec{r}. \end{aligned} \quad (9)$$

Here only transitions from  $d$  sub-bands to the  $s$  band are considered, and therefore  $n_s(\vec{k} + \vec{q}) = 0$ . Replacing the summation over  $k$  by an integration and using the parabolic-band approximation for the energy values, the diagonal part of Eq. (9) becomes

$$\begin{aligned} \epsilon_{ds}^{\sigma}(\vec{q} + \vec{G}) &= v(\vec{q} + \vec{G}) \frac{4m_{s\sigma}}{\pi\hbar^2} \sum_m \int_0^{k_{Fdm\sigma}} dk k^2 \\ &\times \int_0^{\pi} \int_0^{2\pi} \frac{|y_2^m(\theta_{k-G}, \phi_{k-G})|^2 [F_2(|\vec{k} - \vec{G}|)]^2}{(m_{s\sigma}/m_{dm\sigma} - 1)k^2 - q^2 - 2kq \cos\theta_{kq}} \\ &\times \sin\theta_k d\theta_k d\phi_k, \end{aligned} \quad (10)$$

where  $y_2^m(\theta, \phi)$  are spherical harmonics,  $\theta_{k-G}$ ,  $\phi_{k-G}$  are the zenith and azimuthal angles, respectively, of the vector  $\vec{k} - \vec{G}$  and  $\theta_{kq}$  is the angle between the vectors  $\vec{k}$  and  $\vec{q}$ . The coordinate system and  $F_2(\vec{k})$  are the same as defined in PJ. For  $\vec{G} = 0$ , the angular integration in Eq. (10) can be carried out exactly for a general direction of  $\vec{q}$  using the rotation matrices as discussed in PJ. This simplifies Eq. (10) to

$$\epsilon_{ds}^{\sigma}(\vec{q} + \vec{G}, \vec{q}) = v(\vec{q} + \vec{G}) \frac{4m_{s\sigma}}{\pi\hbar^2} \sum_m \int_0^{k_{Fdm\sigma}} dk k^2 \int_0^{\pi} \int_0^{2\pi} \frac{y_2^m(\theta_{k-G}, \phi_{k-G}) y_2^{*m}(\theta_k, \phi_k) F_2(\vec{k}) F_2(|\vec{k} - \vec{G}|)}{(m_{s\sigma}/m_{dm\sigma} - 1)k^2 - q^2 - 2kq \cos\theta_{kq}} \sin\theta_k d\theta_k d\phi_k. \quad (14)$$

To simplify Eq. (14) further, we calculated the diagonal part  $\epsilon_{ds}^{\sigma}(\vec{q} + \vec{G})$  explicitly. We again calculated  $\epsilon_{ds}^{\sigma}(\vec{q} + \vec{G})$  for the  $m=0$   $d$  sub-band using an effective mass  $m_{dm\sigma}^{\text{av}}$  which is the simple average of the effective masses of all the five  $d$  sub-bands, and multiplied it by a weight factor  $W$  which is the

$$\begin{aligned} \epsilon_{ds}^{\sigma}(\vec{q}) &= v(q) \frac{4m_{s\sigma}}{\pi\hbar^2} \sum_m (-1)^m \\ &\times \left( \int_0^{k_{Fdm\sigma}} dk [F_2(\vec{k})]^2 k^2 [D_{0m}^2 D_{0-m}^2 I_0 \right. \\ &\quad + (D_{1m}^2 D_{-1-m}^2 + D_{-1m}^2 D_{1-m}^2) I_1 \\ &\quad \left. + (D_{2m}^2 D_{-2-m}^2 + D_{-2m}^2 D_{2-m}^2) I_2 \right], \end{aligned} \quad (11)$$

where  $D_{mm'}^2$  are the elements of the rotation matrix with argument  $(-\gamma, -\beta, -\alpha)$ .  $\alpha, \beta, \gamma$  are the Euler angles.  $I_0, I_1, I_2$  are the same as given in PJ.

For nonzero values of  $\vec{G}$ , Eq. (10) is evaluated for  $\vec{q}$  along the  $Z$  direction. The analytical integration over  $\phi_k$  is made by the method of partial fractions. Equation (10) becomes

$$\begin{aligned} \epsilon_{ds}^{\sigma}(\vec{q} + \vec{G}) &= v(\vec{q} + \vec{G}) \frac{4m_{s\sigma}}{\pi\hbar^2} \sum_m (-1)^m \int_0^{k_{Fdm\sigma}} dk k^2 \\ &\times \left( (48)^2 \sum_i \sum_j a_i a_j \alpha_i \alpha_j \right. \\ &\quad \left. \times \int_0^{\pi} \frac{I_m(k, \theta_k) \sin\theta_k d\theta_k}{(m_{s\sigma}/m_{dm\sigma} - 1)k^2 - q^2 - 2kq \cos\theta_k} \right), \end{aligned} \quad (12)$$

where

$$\begin{aligned} I_m(k, \theta_k) &= \int_0^{2\pi} \frac{P_2^m(\cos\theta_{k-G}) P_2^{-m}(\cos\theta_{k-G}) |\vec{k} - \vec{G}|^4}{(|\vec{k} - \vec{G}|^2 + \alpha_i^2)^4 (|\vec{k} - \vec{G}'|^2 + \alpha_j^2)^4} d\phi_k. \end{aligned} \quad (13)$$

Substituting the values of the Legendre polynomials for different magnetic quantum numbers, the integrals in Eq. (13) are evaluated by the method of partial fractions. The final expressions are very lengthy and are not presented here. The integrals over  $k$  and  $\theta_k$  are carried out numerically by the Gauss quadrature method.

It is not possible to evaluate analytically the nondiagonal part of  $\epsilon_{ds}^{\sigma}(\vec{q} + \vec{G}, \vec{q} + \vec{G}')$  in the present noninteracting-spin band scheme. To estimate the nondiagonal part, we substitute  $\vec{G}' = 0$  into Eq. (9) and take the nonzero values of  $\vec{G}$ . Equation (9) becomes

number of active  $d$  sub-bands. We found that these two calculations agree within  $\pm 7\%$ . Therefore, we put  $m=0$ , replace  $m_{dm\sigma}$  by  $m_{dm\sigma}^{\text{av}}$ , and multiply Eq. (14) by  $W$ . This approximation may not have too much weight for a first estimate of the local-field corrections due to interband transitions. Choos-

ing  $\vec{q}$  along the  $Z$  direction Eq. (14) simplifies to

$$\epsilon_{ds}^{\sigma}(\vec{q} + \vec{G}, \vec{q}) = v(\vec{q} + \vec{G}) \frac{4Wm_{s\sigma}}{\pi\hbar^2} \int_0^{k_{Fds\sigma}} dk k^2 F_2(\vec{k}) I(k), \quad (15)$$

where  $I(k)$  is a function of  $k$  and is obtained after integrating over  $\theta_k$ . The final expression is very lengthy and is not presented here.

A similar calculation is carried out for  $\epsilon_{sd}^{\sigma}$ . When  $\vec{G} = \vec{G}' = 0$ ,

$$\begin{aligned} \epsilon_{sd}^{\sigma}(\vec{q}) = v(\vec{q}) \frac{4}{\pi\hbar^2} \sum_m (-1)^m m_{dm\sigma} \\ \times \left( D_{0m}^2 D_{0-m}^2 \int_0^{k_{Fs\sigma}} I_0' k^2 dk \right. \\ + (D_{-1m}^2 D_{1-m}^2 + D_{1m}^2 D_{-1-m}^2) \int_0^{k_{Fs\sigma}} I_1' k^2 dk \\ \left. + (D_{-2m}^2 D_{2-m}^2 + D_{2m}^2 D_{-2-m}^2) \int_0^{k_{Fs\sigma}} I_2' k^2 dk \right). \end{aligned} \quad (16)$$

The expressions for  $I_0'$ ,  $I_1'$ , and  $I_2'$  can be written just by replacing  $\vec{p}$  by  $\vec{q}$  in Eqs. (41), (43), and (44) of PJ, respectively. When  $\vec{G} = \vec{G}' \neq 0$ ,

$$\begin{aligned} \epsilon_{sd}^{\sigma}(\vec{q} + \vec{G}) = v(\vec{q} + \vec{G}) \frac{4}{\pi\hbar^2} \sum_m (-1)^m m_{dm\sigma} \int_0^{k_{Fs\sigma}} dk k^2 \\ \times \left( (48)^2 \sum_{i=1}^4 \sum_{j=1}^4 a_i a_j \alpha_i \alpha_j \right. \\ \left. \times \int_0^{\pi} \frac{I_m'(k, \theta_k) \sin \theta_k d\theta_k}{(m_{dm\sigma}/m_{s\sigma} - 1)k^2 - q^2 - 2kq \cos \theta_k} \right). \end{aligned} \quad (17)$$

The analytical expression for  $I_m'(k, \theta_k)$  can be obtained by replacing  $|\vec{k} - \vec{G}|$  by  $|\vec{k} + \vec{q} + \vec{G}|$  in Eq. (13) and is evaluated in the same way as  $I_m(k, \theta_k)$ .

The nondiagonal part of  $\epsilon_{sd}^{\sigma}$  is

$$\epsilon_{sd}^{\sigma}(\vec{q} + \vec{G}, \vec{q}) = v(\vec{q} + \vec{G}) \frac{4Wm_{dm\sigma}^{av}}{\pi\hbar^2} \int_0^{k_{Fs\sigma}} dk k^2 I'(k), \quad (18)$$

where  $I'(k)$  is again a complicated and lengthy function of  $k$  involving the integration over  $\theta_k$  and is not presented here. [The final expressions for  $I_m(k, \theta_k)$ ,  $I_m'(k, \theta_k)$ ,  $I(k)$ , and  $I'(k)$  may be obtained on request.]

#### IV. CALCULATIONS AND RESULTS

The dielectric function was calculated using Eqs. (5), (7), (8), (11), (12), and (15)–(18). First we calculated  $\epsilon(\vec{q}, \vec{q})$  along the three principal symmetry directions [100], and [110], and [111], fol-

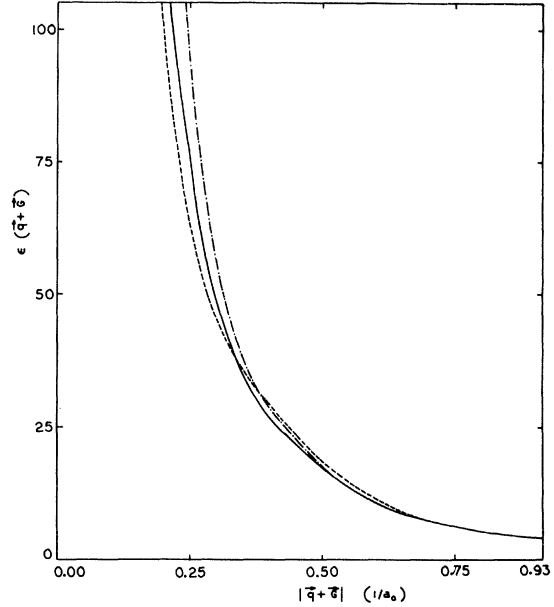


FIG. 2.  $\epsilon(\vec{q})$  vs  $\vec{q}$  for ferromagnetic nickel. The solid, dashed-dot, and dashed lines represent the dielectric function along [100], [110], and [111] directions, respectively.

lowing the procedure discussed in PJ for  $\vec{q}$  in the first Brillouin zone. The results are shown in Fig. 2. We find that the anisotropy is small except in the vicinity of  $\vec{q} = 0$ . We calculated  $\epsilon(\vec{q} + \vec{G})$  for  $\vec{q}$  along the [001] direction. Since the electron-electron interaction potential  $v(\vec{q} + \vec{G})$  greatly enhances the dielectric function for small values of  $|\vec{q} + \vec{G}|$  while  $v(\vec{q} + \vec{G})$  greatly suppresses it for large values of  $|\vec{q} + \vec{G}|$ , we plot the results for  $\chi(\vec{q} + \vec{G})$  defined as  $[\epsilon(\vec{q} + \vec{G}) - 1]/v(\vec{q} + \vec{G})$  to see the band-structure effects more transparently. These results are shown in Fig. 3.  $\chi(\vec{q} + \vec{G})$  essentially is the polarizability function. We also plot the intra- and interband parts separately, the intraband part being defined as  $\sum_{\sigma} (\chi_{ss}^{\sigma} + \chi_{dd}^{\sigma})$  for  $m = m'$  and interband part being defined as  $\sum_{\sigma} (\chi_{da}^{\sigma})$  for  $m \neq m' + \chi_{ds}^{\sigma} + \chi_{sd}^{\sigma}$ , while the total polarizability function is the sum of the intra- and interband parts. Here  $\chi_{ss}^{\sigma}$ , etc. are defined as  $\epsilon_{ss}^{\sigma}(\vec{q} + \vec{G})/v(\vec{q} + \vec{G})$ . Because of the nonorthogonality of the  $s$  and  $d$  wave functions, the interband part does not reduce to the correct limit as  $\vec{q} \rightarrow 0$ . However, we have taken it to be zero at  $\vec{q} = 0$ . The interband part shows a peak near  $q = 0.1$  and shows an oscillatory nature for large values of  $|\vec{q} + \vec{G}|$ . Therefore few more broad maxima are found in the total polarizability function. This is a consequence of including the  $d$  band in our calculations.

Using the parameters of PJ, similar calculations are also performed for the diagonal and nondiagonal parts of the dielectric function for the

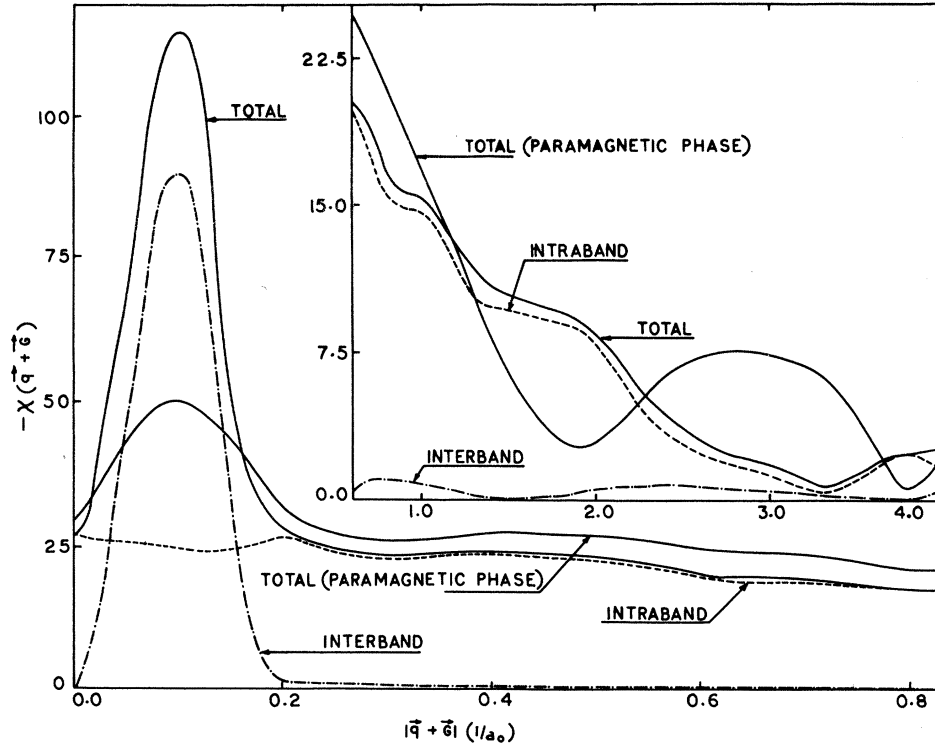


FIG. 3.  $\chi(\vec{q}+\vec{G})$  vs  $|\vec{q}+\vec{G}|$  for ferromagnetic nickel. Solid lines represent the total polarizability function, that is,  $\chi(\vec{q}+\vec{G})$  is the sum of the intraband and interband parts. The intraband part  $\Sigma_{\sigma}(\chi_{ss}^{\sigma} + \chi_{dd}^{\sigma})$  for  $m = m'$  is represented by the dashed line and the interband part  $\Sigma_{\sigma}(\chi_{dd}^{\sigma}$  for  $m \neq m' + \chi_{ds}^{\sigma} + \chi_{sd}^{\sigma})$  is represented by the dash-dot line. In the upper right-hand corner  $\chi(\vec{q}+\vec{G})$  is represented on a magnified scale for  $|\vec{q}+\vec{G}| > 0.6$ .

paramagnetic phase.  $\chi(\vec{q}+\vec{G})$  for the paramagnetic phase for the configuration  $(3d)^{9.4} (4s)^{0.6}$  is also shown in Fig. 3. We find that the polarizability function for the ferromagnetic phase is larger than that for the paramagnetic phase in the low- $|\vec{q}+\vec{G}|$  region, while both are of the same order of magnitude for large values of  $|\vec{q}+\vec{G}|$ .

The relative magnitudes of the various contributions are shown in Table III. We find in our calculations that  $\Sigma_{\sigma} \chi_{dd}^{\sigma}$  is 100 to 20 times larger than  $\Sigma_{\sigma} \chi_{ss}^{\sigma}$  for  $|\vec{q}+\vec{G}|$  between 0.1 and 4.7. The contributions of  $\chi_{ss}^{\sigma}$  and  $\chi_{ss}^{\downarrow}$  are found to be equal because the majority- and minority-spin  $s$  bands almost overlap. The contribution of  $\chi_{ds}^{\downarrow}$  is about

20% larger than that of  $\chi_{ds}^{\uparrow}$  for small values of  $|\vec{q}+\vec{G}|$ , and both are of same order of magnitude for large values of  $|\vec{q}+\vec{G}|$ . The contribution  $\Sigma_{\sigma} \chi_{sd}^{\sigma}$  is only due to minority-spin bands. We note especially that the major contribution is from minority-spin bands because of the partially filled  $d$  sub-bands.

The nondiagonal part of the polarizability function which gives rise to the local-field corrections is shown in Fig. 4. The intra- and interband parts, as defined earlier, and their sum are shown in the figure for the specific value of  $q = 0.2$ . We find that the interband part is oscillatory for large values of  $|\vec{q}+\vec{G}|$ , while both intra- and interband

TABLE III. Relative magnitudes of different contributions to the polarizability function. Here  $|\vec{q}+\vec{G}|$  is in inverse bohr units.

$ \vec{q}+\vec{G} $	$-\chi_{ss}^{\uparrow}$	$-\chi_{ss}^{\downarrow}$	$-\chi_{dd}^{\uparrow}$	$-\chi_{ds}^{\uparrow}$	$-\chi_{ds}^{\downarrow}$	$-\chi_{sd}^{\downarrow}$
0.1	1.33061	1.32875	1345.37463	0.36593	0.32720	-0.05056
0.2	1.32194	1.32010	58.33454	0.37512	0.33770	-0.06002
0.4	1.28654	1.28475	45.48725	0.40005	0.36731	-0.09277
0.6	1.22476	1.22304	39.00742	0.39578	0.36241	-0.18363
1.0	0.99243	0.99108	24.17774	0.56881	0.43831	-0.33477
1.52768	0.35253	0.35199	17.39716	0.80581	0.80472	-0.19875
1.89781	0.21153	0.21111	17.05482	0.61344	0.61259	-0.09413
2.81394	0.09068	0.09022	4.07287	0.23996	0.23996	-0.04557
3.77977	0.04950	0.04950	4.57963	0.05286	0.05286	-0.01259
4.71105	0.03128	0.03128	4.23629	0.02085	0.01043	-0.00261

parts converge smoothly. We further observe that local-field corrections due to interband transitions are negligible as compared with local-field corrections due to intraband transitions for ferromagnetic nickel. By comparison, we find that the nondiagonal part of the polarizability function is of the same order of magnitude as the diagonal part. Therefore we conclude that for large values of  $|\vec{q} + \vec{G}|$  the local-field corrections become quite important.

### V. DISCUSSIONS

Exchange and correlation corrections in the dielectric function for the ferromagnetic phase should be very important. Kim *et al.*<sup>15</sup> calculated the charge susceptibility of a ferromagnetic electron gas including the exchange interaction. They found that the dielectric function for negative-spin electrons becomes negative for small values of  $\vec{q}$  and is singular at a finite value of  $\vec{q}$ , while the dielectric function for positive-spin electrons shows the usual behavior. Hayashi and Shimizu<sup>6</sup> pointed out that the effect of exchange on the impurity screening in ferromagnetic nickel is negligible. However, the exact form of the exchange-correlation corrections for  $d$  electrons is not well established, and the inclusion of exchange and correlation corrections for  $s$  electrons will have little effect on the total dielectric function, because  $\epsilon_{dd}$  is dominating. Therefore we carried out the calculations in the Hartree approximation to investigate the local-field corrections in a transition metal in the ferromagnetic phase.

The noninteracting-spin band model is a rather simplified picture of the complicated ferromagnetic-nickel system. We have completely neglected the  $s$ - $d$  hybridization which splits the  $s$  and  $d$  bands. However, this splitting is in a small region of momentum space and well below the Fermi energy. Again, in principle we should use a wave function for the  $s$  electrons which is orthogonal to the core as well as to the  $d$ -wave functions. An orthogonalized plane wave is a suitable choice, but it was found that these orthogonalization corrections are comparatively very small, and therefore a plane-wave approximation for the wave function and a parabolic-band approximation for the energy values of the  $s$  electrons are fairly justified. On the other hand, the parabolic-band approximation for  $d$  electrons is very crucial. However, the present model band structure in-

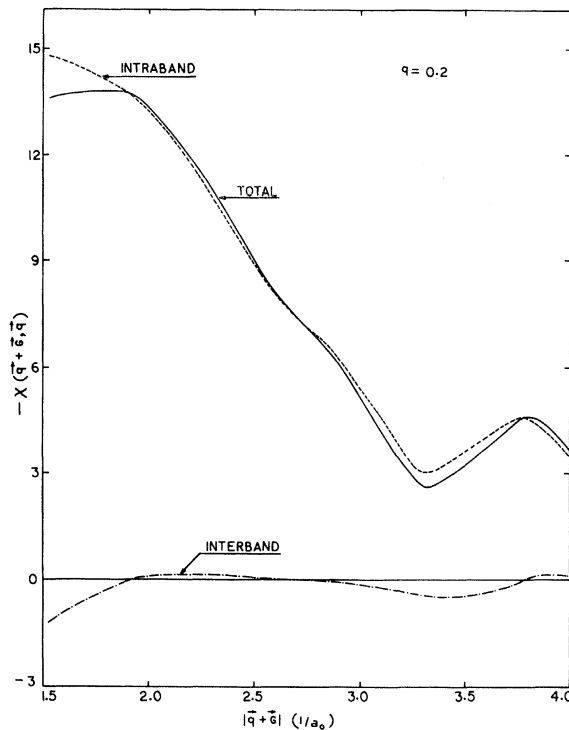


FIG. 4.  $\chi(\vec{q} + \vec{G}, \vec{q})$  vs  $|\vec{q} + \vec{G}|$  for ferromagnetic nickel. The dashed line represents the intraband part and the dashed-dot line represents the interband part. The solid line represents the sum of these two.

cludes all the essential features of the detailed band-structure calculations. The general behavior of the polarizability function is the same for both the paramagnetic and ferromagnetic phases in the Hartree approximation. Our main emphasis has been on a quantitative estimate of the local-field corrections in a transition metal using a multi-band-model band structure. We conclude that these effects are quite important for large values of  $|\vec{q} + \vec{G}|$  and should be included in the calculation of any physical property of these metals.

### ACKNOWLEDGMENT

The authors acknowledge helpful discussions with Professor S. K. Joshi, Dr. K. N. Pathak, and Professor S. K. Sinha. Financial assistance from the Council of Scientific and Industrial Research and University Grants Commission is also acknowledged.

<sup>1</sup>S. L. Adler, Phys. Rev. **126**, 413 (1962).

<sup>2</sup>N. Wiser, Phys. Rev. **129**, 62 (1963).

<sup>3</sup>H. Ehrenreich and M. H. Cohen, Phys. Rev. **115**, 786

(1959).

<sup>4</sup>S. K. Sinha, R. P. Gupta, and D. L. Price, Phys. Rev. Lett. **26**, 1324 (1971); S. K. Sinha, Phys. Rev. **177**,

- 1256 (1969).
- <sup>5</sup>S. K. Sinha, R. P. Gupta, and D. L. Price, Phys. Rev. B (to be published). We are sincerely thankful to Professor S. K. Sinha for sending us a preprint of the paper.
- <sup>6</sup>E. Hayashi and M. Shimizu, J. Phys. Soc. Jpn. 26, 1396 (1969); 27, 43 (1969).
- <sup>7</sup>S. Prakash and S. K. Joshi, Phys. Rev. B 2, 915 (1970).
- <sup>8</sup>S. Prakash and S. K. Joshi, Phys. Rev. B 4, 1770 (1971).
- <sup>9</sup>W. Hanke and H. Bilz, in *Neutron Inelastic Scattering* (International Atomic Energy Agency, Vienna, 1972), p. 3.
- <sup>10</sup>W. Hanke, Phys. Rev. B 8, 4585 (1973).
- <sup>11</sup>W. Hanke, Phys. Rev. B 8, 4591 (1973).
- <sup>12</sup>J. Singh, N. Singh, and S. Prakash (unpublished).
- <sup>13</sup>R. J. Birgeneau, J. Cordes, G. Dolling, and A. D. B. Woods, Phys. Rev. 136, A1359 (1964).
- <sup>14</sup>J. W. D. Connolly, Phys. Rev. 159, 415 (1967); S. Wakoh and J. Yamashita, J. Phys. Soc. Jpn. 19, 1342 (1964); E. I. Zornberg, Phys. Rev. B 1, 244 (1970); J. Callaway and C. S. Wang, Phys. Rev. B 7, 1096 (1973).
- <sup>15</sup>D. J. Kim, B. B. Schwartz, and H. C. Praddaude, Phys. Rev. B 7, 205 (1973).